

# PROCEEDINGS OF SPIE

[SPIDigitalLibrary.org/conference-proceedings-of-spie](https://spiedigitallibrary.org/conference-proceedings-of-spie)

## Chebyshev gradient polynomials for high resolution surface and wavefront reconstruction

Maham Aftab, James H. Burge, Greg A. Smith, Logan Graves, Chang-jin Oh, et al.

Maham Aftab, James H. Burge, Greg A. Smith, Logan Graves, Chang-jin Oh, Dae Wook Kim, "Chebyshev gradient polynomials for high resolution surface and wavefront reconstruction," Proc. SPIE 10742, Optical Manufacturing and Testing XII, 1074211 (14 September 2018); doi: 10.1117/12.2320804

**SPIE.**

Event: SPIE Optical Engineering + Applications, 2018, San Diego, California, United States

# Chebyshev Gradient Polynomials for High Resolution Surface and Wavefront Reconstruction

Maham Aftab<sup>a</sup>, James H. Burge<sup>a</sup>, Greg A. Smith<sup>a</sup>, Logan Graves<sup>a</sup>, Chang-jin Oh<sup>a</sup>,  
Dae Wook Kim<sup>\*a,b</sup>

<sup>a</sup>College of Optical Sciences, University of Arizona, 1603 E. University Blvd., Tucson, AZ 85721,  
USA

<sup>b</sup>Steward Observatory, University of Arizona, 933 N. Cherry Ave., Tucson, AZ 85719, USA

## ABSTRACT

A new data processing method based on orthonormal rectangular gradient polynomials is introduced in this work. This methodology is capable of effectively reconstructing surfaces or wavefronts with data obtained from deflectometry systems, especially during fabrication and metrology of high resolution and freeform surfaces. First, we derived a complete and computationally efficient vector polynomial set, called **G** polynomials. These polynomials are obtained from gradients of Chebyshev polynomials of the first kind – a basis set with many qualities that are useful for modal fitting. In our approach both the scalar and vector polynomials, that are defined and manipulated easily, have a straightforward relationship due to which the polynomial coefficients of both sets are the same. This makes conversion between the two sets highly convenient. Another powerful attribute of this technique is the ability to quickly generate a very large number of polynomial terms, with high numerical efficiency. Since tens of thousands of polynomials can be generated, mid-to-high spatial frequencies of surfaces can be reconstructed from high-resolution metrology data. We will establish the strengths of our approach with examples involving simulations as well as real metrology data from the Daniel K. Inouye Solar Telescope (DKIST) primary mirror.

**Keywords:** Surface reconstruction, Surface measurements, Optical metrology, Information processing, Deflectometry, Testing, Modal fitting, Numerical approximation and analysis

## 1. INTRODUCTION

Deflectometry [1-5] is an optical metrology technique particularly effective for the measurement of high-resolution and freeform surfaces. It measures the slope of the test optic surface in a modest package, requiring only a light source and a camera. To obtain the surface sag map from measured slope data, integration must be performed either with a zonal approach such as Southwell integration [6] or a modal one such as proposed in this paper.

In this work we show how our modal reconstruction method, using the proposed Chebyshev gradient polynomials (called **G** polynomials) can work well for large, freeform and especially high-resolution surfaces, such as the Daniel K. Inouye Solar Telescope (DKIST) [7], while also dealing with some common metrology requirements for such projects. Some of these requirements are a large dynamic range of slopes and local obscurations from small fiducials commonly placed on the surface of the mirror during its testing. These fiducials are used as reference markers and can significantly impact the accuracy of surface reconstruction. The DKIST primary mirror is a 4.2 m aperture off-axis parabola. This telescope, which will be to-date the largest optical solar telescope ever built, aims to provide vastly enhanced spatial, spectral and image resolution for solar observation. The surface quality specifications for this project were quite challenging, particularly requirements for the surface figure, irregularity and BRDF (Bidirectional Reflectance Distribution Function). This may be the smoothest large mirror ever made [8]. One big challenge with fabrication of such large, freeform mirrors is that the metrology method requires high dynamic range coupled with excellent resolution and accuracy. Deflectometry proved to be a great metrology tool for the DKIST primary and this paper includes examples of data processing from this mirror.

\*letter2dwk@hotmail.com

Optical Manufacturing and Testing XII, edited by Ray Williamson, Dae Wook Kim,  
Rolf Rascher, Proc. of SPIE Vol. 10742, 1074211 · © 2018 SPIE  
CCC code: 0277-786X/18/\$18 · doi: 10.1117/12.2320804

Proc. of SPIE Vol. 10742 1074211-1

Surface reconstruction techniques can be divided into two general categories: (a) Zonal methods, such as the Southwell zonal technique, which perform a numerical integration zone by zone and takes a localized approach to the measurement data and (b) Modal methods, such as the one with **G** polynomials, which reconstruct data using polynomial fitting and looks at the data over the entire aperture in one go. Both methods have their pros and cons. Generally, several factors such as processing speed, need for high-resolution data fitting and type of aperture etc. affect the choice of the surface / wavefront reconstruction technique. Modal methods are generally less sensitive to measurement noise and the number of modes or polynomials used can be adapted to the situation at hand [9]. Li et al. [10] discuss a zonal integration method for deflectometry that shows better results than the traditional Southwell zonal integration method, but it still underperforms compared to modal fitting in terms of reconstructed surface errors. Results from different modal methods may also vary as the type of polynomials used can have different effects. It is usually preferable to use orthogonal polynomial basis sets for many reasons [11].

We introduced the vector polynomials set (called **G** polynomials), orthogonal over a rectangular pupil and its associated modal fitting method in [12]. In this work, we expand on that method and show some of its other applications and advantages. It is important to note that this technique was not developed to be a representation of balanced aberrations over a rectangular aperture. We do not aim to provide a modal solution to optical design problems where aberration analysis, based on the coefficients of the polynomial set, is critical. Instead, we use this method as an alternative to zonal integration, for the reasons discussed in [12]. Furthermore, the optical systems under consideration in [12] and also in this work are neither rotationally symmetric nor anamorphic.

More and more optical systems are now seen to be employing rectangular apertures. Some examples are the Gaia telescope system [13, 14] and X-ray mirrors [15]. Many imaging applications may need to utilize the full detector size, which generally has a rectangular format. Although **G** polynomials are optimal for fitting rectangular datasets because of their orthogonality across them, the method is general enough to reconstruct other datasets. It may be particularly useful for non-symmetric or freeform shapes. This methodology also shows great results in the presence of markers such as fiducials used during deflectometry measurements or blockers such as telescope spiders. It also works well for cases where the wavefront is sampled non-traditionally such as uneven sampling in the  $x$  and  $y$  directions.

We start with a recap of the Chebyshev gradient polynomials basis set upon which the reconstruction technique is based, in Section 2, describing the development and advantages of these polynomials. Next, in Section 3, we provide an overview of deflectometry systems and specifically metrology of the DKIST primary mirror. Also explained are some properties of deflectometry and the DKIST mirror that could benefit from the **G** polynomials data processing technique. Section 4 provides specific cases of surface reconstruction and an evaluation of the **G** polynomials fitting technique for those examples. The cases with DKIST data are compared to the traditional Southwell zonal method reconstructions, which was used as the standard reconstruction technique for deflectometry measurements. The conclusion is presented in Section 5.

## 2. MODAL BASIS FOR SURFACE / WAVEFRONT RECONSTRUCTION

The foundation of this data fitting methodology lies in the modal basis set used. Two dimensional Chebyshev polynomials were chosen as the scalar basis set (called F polynomials), the gradient of which is used as the vector polynomial set (called **G** polynomials). F polynomials are obtained by the product of two one dimensional Chebyshev polynomials (called T polynomials). Eqn.1 is a mathematical description of the T polynomials and Eqn.2 of the F polynomials and Eqn.3 describes the derivation of the **G** polynomial set.

$$T_{m+1}(x) = 2xT_m(x) - T_{m-1}(x) \quad \text{where } T_0(x) = 1, T_1(x) = x, \quad \text{for } -1 \leq x \leq 1 \quad (1)$$

$$F_n^m(x, y) = T_m(x)T_n(y) \quad (2)$$

$$\vec{G}_n^m(x, y) = \nabla F_n^m(x, y) = \frac{\partial}{\partial x} F_n^m(x, y) \hat{i} + \frac{\partial}{\partial y} F_n^m(x, y) \hat{j} \quad (3)$$

Chebyshev polynomials were used as the basis for modal fitting for a variety of reasons, one of the most important one being their orthogonality across rectangular pupils [16]. Ref [12] lists many other qualities of Chebyshev polynomials

that make them an attractive option for data fitting such as the fact that in many cases their discrete orthogonality holds exactly.

We demonstrated that the gradients of the  $F$  polynomials set (i.e.  $G$  polynomials) are also orthogonal over rectangular apertures [12]. This is an exciting prospect as many vector polynomial sets, derived from orthogonal scalar polynomials, do not hold orthogonality over the specified aperture and must be orthogonalized, using a procedure such as the Gram-Schmidt orthogonalization process [17]. For example, this is the case for Zernike based rectangular gradient polynomials [18]. Although these polynomials have advantages for aberration balancing, we do not require the representation of balanced aberrations, as explained in Section 1. Hence, it is advantageous for our applications to use Chebyshev polynomials. The fact that  $G$  polynomials form an orthogonal set makes data processing and the surface / wavefront reconstruction process much simpler and computationally efficient. Additionally, this is one of the reasons why this methodology can make use of up to hundreds of thousands of polynomials.

The data fitting process is straightforward. Slope data (measured or simulated) can be expanded in terms of the gradient polynomial basis set, to obtain the coefficients of the expansion. These vector polynomial coefficients are then converted to coefficients of the scalar polynomial basis, using the previously derived relationship between the two [12]. Finally, using the scalar polynomial coefficients and the corresponding polynomial terms, the wavefront or surface is obtained. A great feature of the modal fitting method using  $G$  polynomials is that the relationship between scalar and vector polynomial coefficients is one-to-one. In other words, the scalar polynomial coefficients are the same as their vector polynomial coefficient counterparts. This further improves the accuracy and computational efficiency of the fit, especially when a large number of polynomial terms are involved. Lastly, it is worth mentioning that recursive relationships for generating both scalar and vector polynomial sets ( $F$  and  $G$  respectively) were derived and the error between the exact and recursive forms, even for very high orders, was negligible. Details of the polynomial sets, the mathematical background, data fitting method and properties of all aforementioned topics are detailed in Ref [12].

### 3. METROLOGY OF HIGH-RESOLUTION AND FREEFORM OPTICS

Freeform surfaces have rapidly been gaining popularity as they allow for additional degrees of freedom for optical design and instrumentation. Some advantages of such surfaces include system miniaturization / compactness by allowing for decreased system mass and volume, higher throughput due to reduced component count and innovative designs, better aberration correction and higher image quality and a larger field of view, with constant performance across it. Examples of systems that could greatly benefit from freeform optics include head mounted displays, very compact camera systems, asymmetric solar energy concentrators and segmented extremely large telescopes.

However, the additional degrees of freedom made possible by freeform optics fundamentally increases the positioning uncertainty and makes it challenging to simultaneously meet the requirements for optical form, mid-to-high spatial frequencies, and surface micro-roughness. Manufacturing and testing of precision freeform optics in particular requires metrology systems with a large dynamic range of measurement. Deflectometry is a good solution due to its high accuracy and large dynamic range.

Similarly, deflectometry provides a great option for measurement of high-resolution surfaces, such as telescope mirrors. An example we will use in particular for this work is the primary mirror of the Daniel K. Inouye Solar Telescope (DKIST), which is a 4.2 meter parabolic segment with more than 8 mm peak-to-valley aspheric departure [19]. This mirror was fabricated at the Optical Engineering and Fabrication Facility (OEFF) at the College of Optical Sciences, University of Arizona. Fig.1 is a schematic of a generic reflective deflectometry system, configured for testing a mirror like the DKIST primary. Light from a source, such as a computer monitor for visible wavelengths or a hot tungsten wire for infrared wavelengths, is incident on the test optic. Light reflected from the test mirror is then recorded by a camera or detector. The source is a known pattern e.g. a sinusoidal wave of a certain frequency. By measuring the change in the recorded pattern, which is the reflection of the source off of the test mirror, the local slopes of the test surface can be calculated. As mentioned in the introduction, metrology of this high-resolution, freeform mirror was a challenging task. At various stages during the fabrication process, different deflectometry systems were used for measurements and analysis [20].

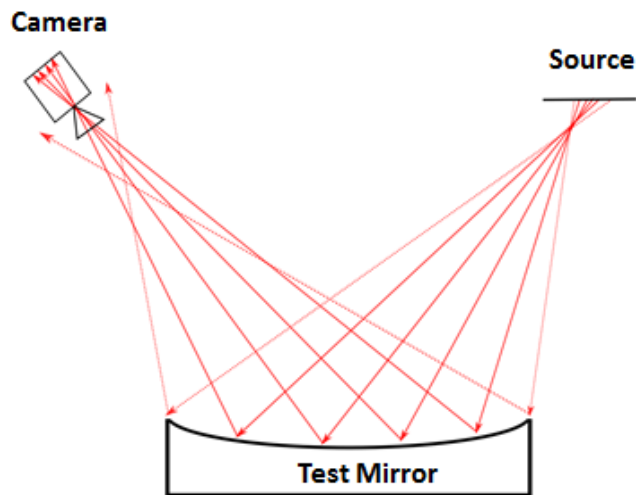


Figure 1. Schematic of a reflective deflectometry set-up.

Deflectometry systems measure the slope of the test surface and have traditionally used Southwell integration for reconstructing the surface being measured. Typically, this works well except in some cases such as when fiducials are placed on the mirror during a metrology run or when there is a scratch on the surface of the optic. Modal methods may work better for surface reconstruction in general under such circumstances, but they often fail to accurately represent high-resolution and freeform surfaces since such surfaces require a very large number of polynomials to be accurately characterized. Using simulated and real data, we show how the **G** polynomial method can overcome this problem as it can use up-to hundreds of thousands of polynomials for surface reconstruction, as required by the specific situation.

## 4. SURFACE RECONSTRUCTION EXAMPLES

This section contains several cases of surface reconstruction that use the **G** polynomials modal method, to highlight some of the situations where this technique can be useful. Also included, where appropriate, are comparisons against the traditional Southwell zonal method.

### 4.1 DKIST surface reconstruction

The Daniel K. Inouye Solar Telescope (DKIST) is a good reference to highlight some of the advantages of the **G** polynomial method. Slope measurements of the DKIST primary mirror were made at the College of Optical Sciences, University of Arizona using deflectometry. This data represents the high-resolution, freeform surface of the mirror. Ref [12] contains reconstruction examples from DKIST data, showing the basic fitting accuracy as well as the accurate representation of the mid-to-high spatial frequencies by comparing high-pass filtered data from the modal reconstruction against the high-pass filtered Southwell reconstructed data, where the Southwell reconstruction is taken as the reference. Here, we will explore a few more examples related to reconstruction of the DKIST surface from its measured deflectometry data and why the **G** polynomials are a good option for this.

First, we take data from the DKIST mirror, over a rectangular aperture, which measures  $\sim 1.84 \times 3.06$  m and contains  $150 \times 250$  pixels, giving it an aspect ratio of 0.6. The data set contains noise, measurement errors etc. that are expected from a real measurement. Fig.2 shows the reconstruction using Southwell zonal method, which is taken as the reference, the **G** polynomial method using 50 polynomials and the difference map between the two surfaces. The difference or error map has a surface RMS of  $8.308 \times 10^{-3} \mu\text{m}$ , which is 0.133% of the reference surface RMS. This shows a good agreement between the two methods, even for a rectangular data set with a relatively large difference between the length and width of the aperture (i.e., a small aspect ratio). From this and other examples [12] we can conclude that the **G** polynomials method can accurately reconstruct data over rectangular apertures.

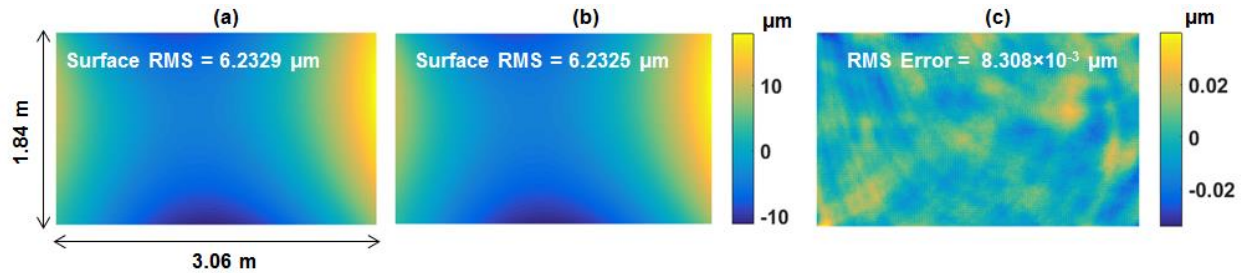


Figure 2. DKIST surface over a  $1.84 \times 3.06$  m aperture, reconstructed using (a) Southwell zonal and (b)  $\mathbf{G}$  polynomial methods. (c) Error map between the two reconstructions ((a) – (b)).

For the second example, we use measured DKIST data, similar to the first example and add fiducials to it in simulation. The analyzed data had an area of  $225 \times 225$  pixels, which is roughly  $2.76 \times 2.76$  m. Nine blockers (modeling fiducials), each having dimensions of  $6 \times 6$  pixels, corresponding to  $\sim 7.35 \times 7.35$  cm were added to both the reference surface (that used the Southwell method) as well as the slope maps. The slope data with fiducials was reconstructed using both the Southwell and  $\mathbf{G}$  polynomials method and compared. Using 500  $\mathbf{G}$  polynomials, the difference between the Southwell and modal reconstructions is  $0.103 \mu\text{m}$  or  $1.609\%$  of the surface RMS of the Southwell surface. This is shown in Fig.3 with the map of the ideal surface as well as the error map, which is the difference between the Southwell method and  $\mathbf{G}$  polynomial method.

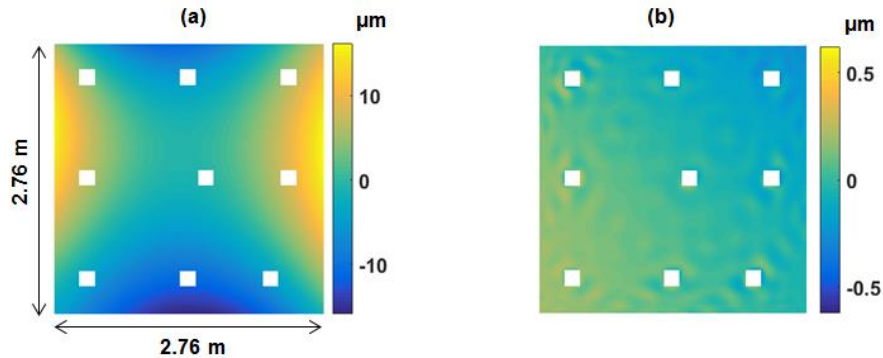


Figure 3. (a) DKIST surface over a  $2.76 \times 2.76$  m aperture, with  $7.35 \times 7.35$  cm fiducials added (in simulation), representing the reference surface. (b) Error between the Southwell method and  $\mathbf{G}$  polynomial reconstruction of the reference surface.

#### 4.2 Reconstruction for unevenly sampled data

Although data is often simulated / measured over equidistance points in both  $x$  and  $y$  directions and the sampling for the two directions is also the same (i.e., the same sampling in  $y$  as in  $x$ ), there may be several situations where this is not the case such as with non-square detector pixels or the presence of astigmatism in the camera lens. In these cases, non-uniform sampling in either or both directions or different sampling in the  $x$  and  $y$  directions may be required. We will investigate both types of situations using simulated data, and assess how well the reconstructions using the  $\mathbf{G}$  polynomial modal method perform in such instances.

For the first example, we generate data over a square pupil, representing a  $2 \times 2$  cm aperture, with a sampling of  $500 \times 300$  points. The ideal, simulated, noise-free surface sag is described by Eqn.4.

$$z = 0.15y^2 + 1.4x^4 - 0.2(x^3 + xy^2) + 0.3y^5 + 1 \times 10^{-3}x^{11} - (xy)^{18} \quad (4)$$

After obtaining  $x$  and  $y$  gradients of the data numerically, surface reconstruction is performed using the  $\mathbf{G}$  polynomials. Fig.4 shows the ideal data, as well as the difference map between the ideal and reconstructed surfaces, when 250  $\mathbf{G}$  polynomials are used. RMS of the simulated surface is  $0.403 \mu\text{m}$  while the RMS of the error map using is  $1.35 \times 10^{-3} \mu\text{m}$  or  $0.33\%$  relative to the ideal surface RMS. It must be noted that since we are using slope data, the mean (representing the piston) is subtracted from the ideal surface as well as its reconstruction.

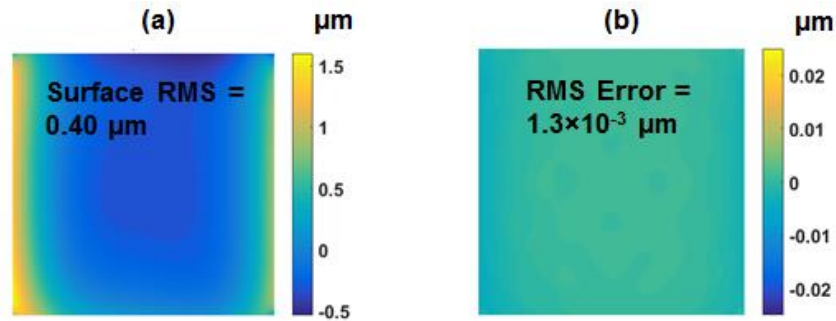


Figure 4. (a) Simulated, ideal surface map (reference) (b) Error between the reference and  $\mathbf{G}$  polynomial generated surface.

In the second example, sampling was kept the same for the  $x$  and  $y$  directions but the sampling along the aperture was changed. Over a  $2 \times 2$  cm aperture, the first 1.25 cm was sampled with 150 points, making the sampling  $1/120$  cm. The remaining 0.75 cm was also sampled with 150 points, making the sampling in this section  $1/200$  cm. Data was simulated over the entire aperture, using Eqn. 4. This gradient data was then reconstructed using the  $\mathbf{G}$  polynomial modal method. The simulated surface RMS is  $0.392 \mu\text{m}$  and the modal method error RMS, using 250 polynomials, is  $2.66 \times 10^{-3} \mu\text{m}$ , or 0.68% relative to ideal surface RMS. Once again, the mean is subtracted from both the ideal surface and its reconstruction. Fig.5 shows the ideal surface map, with an estimation of the regions of different sampling. The error maps between the ideal surface and its  $\mathbf{G}$  polynomial based reconstruction is also shown.

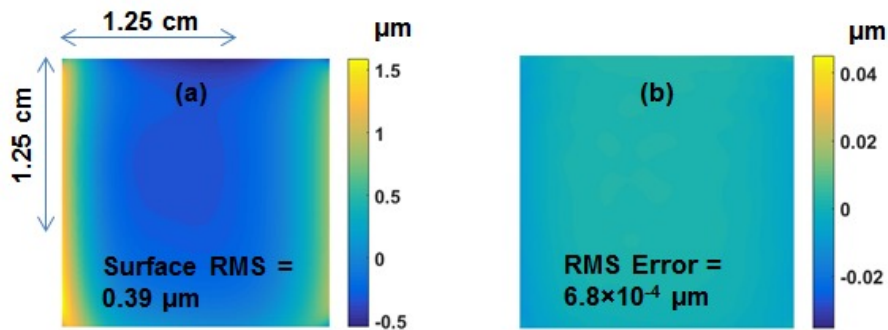


Figure 5. (a) Simulated, ideal surface map (reference). The blue double ended arrows mark the approximate region on the map ( $1.25 \times 1.25$  cm) with a lower sampling (b) Error between the reference and  $\mathbf{G}$  polynomial generated surface.

## 5. CONCLUSION

This paper builds upon the newly developed  $\mathbf{G}$  polynomials modal method for surface / wavefront reconstruction. We provide a brief summary of this method that uses the gradients of Chebyshev polynomials, which are orthogonal over a rectangular aperture. We reiterate the properties of this polynomial set and its attractive ability of being able to generate hundreds of thousands of polynomial terms, which is necessary for the correct representation of high-resolution and freeform surfaces. Since this vector polynomial fitting methodology reconstructs wavefronts / surfaces from slope data and we place a heavy emphasis on high-resolution surfaces that do not have rotational or anamorphic symmetry, we use examples from deflectometry data. We have also provided an overview of deflectometry concepts and techniques and considered specifically the case of the Daniel K. Inouye Solar Telescope (DKIST) primary mirror metrology. Deflectometry provides high-resolution slope data of this freeform surface. Through examples of DKIST surface reconstruction in different cases, such as when fiducials are placed on it, we highlight some of the advantages of our modal data processing method. Also explored are examples from simulated data which highlight certain situations where this  $\mathbf{G}$  polynomial method could prove to be useful, e.g. with uneven sampling in the two orthogonal Cartesian directions. This methodology can prove to be a very useful tool and along with traditional reconstruction techniques for our examples, such as the Southwell zonal method, it can provide a more accurate and effective tool for surface / wavefront reconstruction from slope data.

## ACKNOWLEDGMENTS

This material is partly based on work performed for the DKIST. DKIST is managed by the National Solar Observatory, which is operated by the Association of Universities for Research in Astronomy Inc. under a cooperative agreement with the National Science Foundation. Also, it is based in part upon work performed for the “Post-processing of Freeform Optics” project supported by the Korea Basic Science Institute. The deflectometry related software development is partially funded by the II-VI Foundation Block grant.

## REFERENCES

- [1] Su, P., Parks, R. E., Wang, L., Angel, R. P. and Burge, J. H., "Software configurable optical test system: a computerized reverse Hartmann test," *Appl. Opt.* 49, 4404–4412 (2010).
- [2] Su, T., Park, W. H., Parks, R. E., Su, P. and Burge, J. H., "Scanning long-wave optical test system: A new ground optical surface slope test system," *Proc. SPIE* 8126, 81260E (2011).
- [3] Tang, Y., Su, X., Liu, Y. and Jing, H., "3D shape measurement of the aspheric mirror by advanced phase measuring deflectometry," *Opt. Express* 16, 15090–15096 (2008).
- [4] Jüptner, W. and Bothe, T., "Sub-nanometer resolution for the inspection of reflective surfaces using white light," *Proc. SPIE* 7405, 740502 (2009).
- [5] Knauer, M. C., Kaminski, J. and Hausler, G., "Phase measuring deflectometry: A new approach to measure specular free-form surfaces," *Proc. SPIE* 5457, 366 (2004).
- [6] Southwell, W.H., "Wave-front estimation from wave-front slope measurements," *J. Opt. Soc. Am.* 70, 998–1006 (1980).
- [7] Daniel K. Inouye Solar Telescope. N.p., n.d. Web. 31 July 2017. <<http://dkist.nso.edu/>>.
- [8] Oh, C., Lowman, A. E., Smith, G. A., Su, P., Huang, R., Su, T., Kim, D. W., Zhao, C., Zhou, P. and Burge, J. H., "Fabrication and Testing of 4.2m off-Axis Aspheric Primary Mirror of Daniel K. Inouye Solar Telescope," *Proc. SPIE* 9912, *Advances in Optical and Mechanical Technologies for Telescopes and Instrumentation II*, 99120O (2016).
- [9] Primot, J., Rousset, G. and Fontanella, J. C., "Deconvolution from wave-front sensing: A new technique for compensating turbulence-degraded images," *J. Opt. Soc. Am. A* 7, 1598–1608 (1990).
- [10] Li, M., Li, D., Jin, C., Yuan, K. E. X., Xiong, Z. and Wang, Q., "Improved zonal integration method for high accurate surface reconstruction in quantitative deflectometry," *Appl. Opt.* 56, F144-F151 (2017).
- [11] Zhao, C. and Burge, J. H., "Orthonormal vector polynomials in a unit circle, Part I: basis set derived from gradients of Zernike polynomials," *Opt. Express* 15, 18014–18024 (2007).
- [12] Aftab, M., Burge, J. H., Smith, G. A., Graves, L., Oh, C.J. and Kim, D. W., "Modal Data Processing for High Resolution Deflectometry", accepted for publication in *International Journal of Precision Engineering and Manufacturing-Green Technology* (March, 2018).
- [13] Els, S., Lock, T., Comoretto, G., Gracia, G., O'Mullane, W., Cheek, N. and Vallenari, A., "The commissioning of Gaia," *Proc. SPIE* 9150, 91500A (2014).
- [14] Polidan, R. S., Breckinridge, J. B., Lillie, C. F., MacEwen, H. A., Flannery, M. R., Dailey, D. R., Baldauf, B., Makowski, D. and Rafanelli, G. L., "An evolvable space telescope for future astronomical missions 2015 update," *Proc. SPIE* 9602, 960207 (2015).
- [15] Su, P., Wang, Y., Burge, J., Kaznatcheev, K. and Idir, M., "Non-null full field X-ray mirror metrology using SCOTS: a reflection deflectometry approach," *Opt. Express* 20, 12393-12406 (2012).
- [16] Zwillinger, D., "Special Functions." *CRC Standard Mathematical Tables and Formulae*. 31st ed. Boca Raton, FL: CRC, 2003. 532-38. Print.
- [17] Apostol, T. M., *Linear Algebra: A First Course, with Applications to Differential Equations* (Wiley, 1997), pp. 111–113.
- [18] Li, M., Li, D., Zhang, C., Wang, K. E. Q. and Chen, H., "Modal wavefront reconstruction from slope measurements for rectangular apertures," *J. Opt. Soc. Am. A* 32, 1916–1921 (2015).
- [19] Huang, R., Su, P. and Burge, J. H., "Deflectometry measurement of Daniel K. Inouye Solar Telescope primary mirror," *Proc. SPIE* 9575, *Optical Manufacturing and Testing XI*, 957515 (2015).
- [20] Kim, D. W., Oh, C.J., Lowman, A., Smith, G. A., Aftab, M. and Burge, J. H., "Manufacturing of super-polished large aspheric/freeform optics," *Proc. SPIE* 9912, *Advances in Optical and Mechanical Technologies for Telescopes and Instrumentation II*, 99120F (2016).